forum acusticum 2026
8-12 September · Graz, Austria

An Axisymmetric Modelling Approach for Predicting Tyre Vibration

K. Saito[1], D.J. Thompson[1], G. Squicciarini[1]

[1]Institute of Sound and Vibration Research, University of Southampton, University Road, SO17 1BJ, Southampton, UK

Abstract

Road traffic noise is a major environmental concern in urban areas due to its adverse health effects. At a steady driving speed of 35-120 km/h, tyre noise is known to be the dominant noise source of automotive noise. The tyre has a multi-layer structure of rubber, steel and textile components. Therefore, a full 3D model is computationally expensive, which prevents repeated simulations. In contrast, simplified tyre wave models show limited accuracy above 300 Hz, which corresponds to the dominant frequency range of pass-by noise. To solve this limitation, this research proposes an axisymmetric FEM approach for the tyre capable of predicting the frequency response in higher frequency bands. As a first step, the model is developed for the tyre alone, uninflated and not mounted on a wheel; inflation and wheel coupling, which raise the modal frequencies, will be addressed in later work. This model consists of two equivalent layers representing the rubber and carcass materials, which enables a significant reduction in computational cost compared with conventional 3D models. In addition, by retaining the fundamental tyre structure, the model can predict frequency responses in the high-frequency range. Validation against experimentally measured tyre frequency responses demonstrates improved agreement in the frequency range above 300 Hz, where previous approaches showed limited accuracy. Therefore, the model provides an efficient tool for evaluating tyre surface vibrations in road-excitation-based tyre noise prediction.

Keywords: *tyre noise, road noise, axisymmetric model*

1. Introduction

Automobiles have become the dominant mode of transportation worldwide, and their increasing use has led to significant environmental challenges, particularly noise pollution in urban areas [1]. Environmental noise exposure has been linked to unfavourable health effects, including increased risks of cardiovascular diseases such as myocardial infarction [2-4]. At typical driving speeds, tyre-road interaction noise has been identified as the dominant source of vehicle exterior noise in the range of 35-120 km/h [5]. Therefore, understanding and predicting tyre vibration is essential for noise mitigation. Previous studies have primarily focused on tyre vibration dominated by rigid radial displacement modes of the belts at low frequency, typically below 300 Hz. Analytical models, such as those developed by Pinnington, successfully predict tyre mobility in this frequency range using a wave model of a circular tyre [6][7]. In addition, Wave Finite Element Method (WFEM) approaches, such as those by Waki et al., have demonstrated good agreement with experimental results for wave propagation phenomena in tyres within this frequency range [8]. However, these approaches are fundamentally limited in the high-frequency range relevant to pass-by noise.

At higher frequencies, tyre vibration behaviour becomes significantly more complex. Kropp et al. reported that belt-bending modes contribute to tyre noise in the higher-frequency range relevant to pass-by noise [9]. In this range, multiple modes are closely spaced and highly damped, resulting in overlapping peaks in the frequency response function. Consequently, conventional modelling approaches struggle to accurately predict tyre mobility above 300 Hz. Although full 3D finite element models with multiple material components in each layer can calculate such complex behaviour, their high computational cost prevents their use in iterative design or parametric studies. The work presented here forms part of a longer study, and at this stage the focus is on the tyre alone: uninflated and not connected to the wheel. This isolates the structural behaviour of the tyre carcass itself before the additional effect of inflation pressure is introduced. This will shift the modal frequencies upwards, so the frequency range of interest for the free, uninflated tyre is correspondingly lower. This study proposes a computationally efficient axisymmetric finite element

Corresponding author: ks1m25@soton.ac.uk

model that bridges the gap between low-cost analytical and numerical models and expensive full 3D simulations. Experimental measurements are conducted under the same boundary conditions to validate the model. The results demonstrate that the proposed model can accurately predict tyre vibration up to 500 Hz, while retaining computational efficiency. Achieving a good agreement up to 500 Hz for the uninflated, free tyre is therefore a promising result, and it provides the basis for extending the model to higher frequencies once inflation and wheel coupling are included.

2. Experimental work

2.1 Experimental set-up

The tyre under test was a Bridgestone 205/55R16, specially prepared for this study without a tread pattern but otherwise retaining the structure and materials of the mass-production tyre. Its driving point mobility was measured for later comparison with the 2D axisymmetric model. The tyre was excited with an impact hammer (PCB 086D05, SN 44296, sensitivity: 0.2361 mV/N), and the response was recorded with an accelerometer (PCB352C22, S/N: LW510060, sensitivity: 1.064 mV/m/s^2), using a Data Physics QUATTRO analyser. The measurements were made on the uninflated tyre, not mounted on a wheel. A free-free boundary condition was achieved by suspending the tyre from the ceiling on low-stiffness strings. The accelerometer was mounted at the centre of the tread, and the tyre was excited close to the same point to obtain the driving-point mobility. The frequency range was 0 – 625 Hz with a resolution of 0.7813 Hz and a time span of 1.28 s.

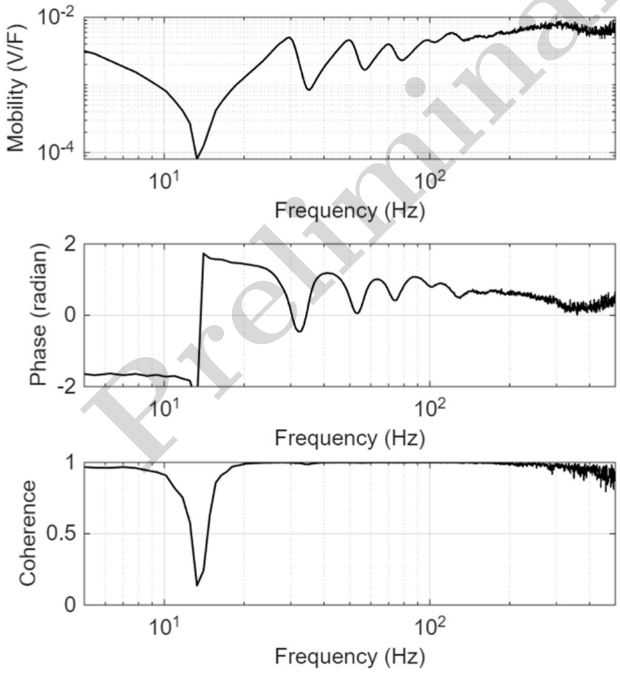

Figure 1. The driving point mobility magnitude (top), phase (middle), and coherence (bottom).

2.2 The measurement results

Figure 1 shows the driving-point mobility of the tyre, excited at the centre of the tread. The magnitude, phase and coherence are presented. The mobility was obtained from the H1 estimator of the frequency response function, averaged over repeated impacts. Apart from the anti-resonance at around 13 Hz, the coherence is close to unity from about 5 Hz to 500 Hz, confirming that the measurement is reliable across this range. Below about 10 Hz, the mobility magnitude follows a decreasing, mass-controlled trend, which is the mass line associated with the suspended free-free configuration of the test. The mobility then shows five distinct peaks below approximately 120 Hz. Above this frequency, the response merges into a single broad peak, which most likely conceals the contribution of several closely spaced and highly damped modes that cannot be individually resolved from the driving point alone.

3. 2D Axisymmetric element model

A tyre is a complex structure built from multiple layers of rubber, fibre and steel, each with different mechanical properties. This layered construction is illustrated, for example, by the detailed model of O'Boy and Dowling, who represented a Dunlop tyre structure using a 3D viscoelastic multilayer model with nine different components [10]. Their model comprised, from the inside outwards: an inner rubber layer, two axial ply cords (fibre), two breaker cords (steel), one bandage cord (fibre), an outer rubber layer, and the tread rubber. Each component differs in thickness, orientation and material, and the layers are stacked on top of one another.

Because a tyre is essentially a cylindrical structure, its 3D modal behaviour can be approximated using a 2D axisymmetric model of the cross-section: the cross-sectional modes are computed on the r-z plane and then expanded over the circumferential direction for each order. For this study, the detailed layered construction was simplified to five components, combining the individual rubber and carcass layers into: top rubber,

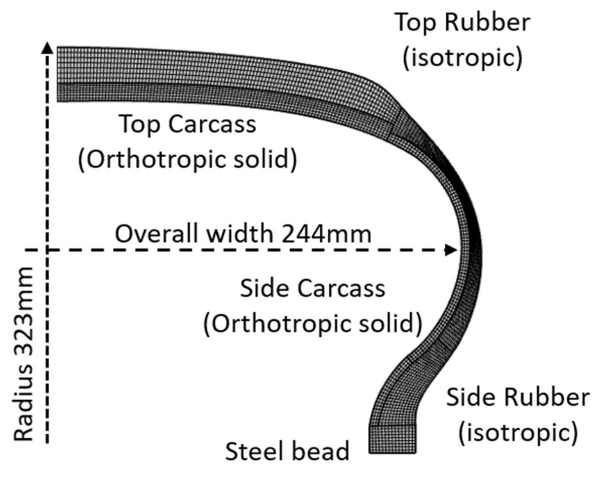

Figure 2. Cross-section of the 2D axisymmetric simplified tyre model.

side rubber, top carcass, side carcass, and steel bead. Together, this simplification and the axisymmetric approach greatly reduce the computational cost and make it easier to identify the mechanical parameters governing each mode.
The tyre modelled here was the Bridgestone 205/55R16 supplied for the measurements. From the inside outwards, its carcass comprises one axial ply, two breaker cords at approximately 30 ° to the circumferential direction, one circumferential bandage cord, and outer rubber layers. The 2D axisymmetric cross-section, built in COMSOL Multiphysics (Figure 2), reproduces this geometry in simplified form. The tread carcass, which includes one axial ply, two breaker cords and one bandage, was combined into a single component, as were the two ply cords of the side carcass. Similarly, the several tread rubber layers were merged into one, and each sidewall was represented by a single rubber material. The rubber and steel bead were defined as isotropic materials, while the tread and side carcass components were given orthotropic properties to represent their cord reinforcement. Each group of layers is thus represented by an equivalent material with effective (smeared) properties that capture the combined stiffness and mass of its parts, avoiding the need to model every layer explicitly.
The mesh was generated with quadrilateral elements throughout, with a maximum element size of 1 mm. The final mesh contained 6132 elements distributed across the five material domains, with an average element quality of 0.914. This model was then used to compute the natural frequencies and mode shapes for different circumferential orders, from which the driving-point mobility was calculated.

4. Results and discussion

4.1 The calculation of mobility

The 2D axisymmetric element model calculates the natural frequencies and mode shape vectors on the r-z plane for each circumferential order; these can then be expanded in the circumferential direction from 0 to 360 degrees. The circumferential orders are calculated up to order 20 in this study, and the calculation frequency range is extended up to 1000 Hz at each circumferential order. The mobility is calculated from the natural frequencies and mode shapes using the modal summation approach.
To correspond with results of the measurements conducted under free-free conditions, the model's boundary conditions are also set to free-free conditions. The natural frequencies and mode shapes are calculated in COMSOL Multiphysics using the eigenfrequency solver. The results are obtained for each azimuthal mode number from 0 to 20, and each mode's mobility and the modal summation are calculated in MATLAB.
The calculation results are shown in Figure 3. These results are obtained by the modal summation with all calculation modes. The red line shows the mobility from

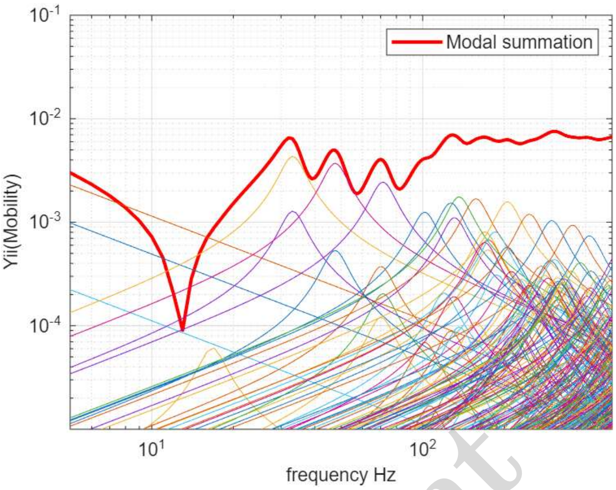

Figure 3. The mobility calculated by the 2D axisymmetric element model from Figure 2 and the results of modal summation.

the modal summation, and the other lines show each mode’s mobility.
The mode at 31 Hz has 2 antinode points in the cross-section and an azimuthal mode number of 2. Below this frequency, there are mass lines from the rigid modes. In addition, the peaks at 46 Hz, 68 Hz, and 124 Hz are detected from the modal summation results. Each of these modes has the same cross-sectional shape, but a different azimuthal mode number. The mode at 46 Hz is azimuthal mode number 3, and the mode at 68 Hz is azimuthal mode number 4.
On the other hand, the peak at 124 Hz is not dominated by a single mode. Around this peak, there are several modes. One is a mode with 2 antinode points in this cross-section, azimuthal order 6, and two other modes have 4 antinode points in this cross-section. The azimuthal orders are 2 and 3. Therefore, the peak at 124 Hz is affected by these different mode shapes. Above this peak, the modal overlap is large, making it difficult to detect individual peaks.

4.2 The parameter fitting

Sensitivity analysis is applied to this model to determine which material properties have the most effect on the natural frequencies of each mode. The measurement results are used as the target. The low-frequency regime is dominated by the modes with 2 antinodes in the cross-section, each with a different azimuthal order. In addition, above 100 Hz, the modes with 4 or more antinodes on the cross-section occur. The sensitivity of each natural frequency to the different material parameters, signified by material parameter ζ is calculated by the following equation:

$$\frac{\partial \omega_l}{\partial \xi} = -\frac{\mathbf{u_l}^* \left(\omega^2 \frac{\partial \mathbf{M}}{\partial \xi} - \frac{\partial \mathbf{K}}{\partial \xi}\right) \mathbf{u_l}}{\mathbf{u_l}^* (2\omega \mathbf{M})\, \mathbf{u_l}} \qquad (1)$$

where ω_l is the natural angular frequency of mode l, $\mathbf{u_l}$ is the corresponding mode shape vector, and $\mathbf{u_l}^*$ indicates the complex conjugate transpose of $\mathbf{u_l}$. $\mathbf{M}$

and **K** are the mass and stiffness matrices. The sensitivity analysis focuses on the material parameters of the carcass components. These materials are orthotropic and are defined using three elastic moduli (E1, E2, E3), three shear moduli (G12, G23, G31), and three Poisson's ratios ($\upsilon 12$, $\upsilon 23$, $\upsilon 31$). Using equation (1), the effect of each parameter on each mode's natural frequency is calculated, and the model is then adjusted to determine the parameters that minimise the difference in peak frequencies compared to the experimental values.

4.3 Comparison between measurement results and calculation results

The calculation results from the 2D axisymmetric model and measurement data under the same boundary conditions are compared in Figure 4. The model parameters were obtained by parameter fitting, as described above. The red line shows the calculation results of the 2D axisymmetric model, and the black dotted line shows the measurement result. The calculated magnitude results agree well with the measured data up to 500 Hz, and each peak frequency and magnitude fit the results. The mobility above 500 Hz cannot be compared with the experimental data because the coherence was insufficient. In addition, the phase results agree with the measurement results. The calculations use the same damping loss factor for all modes. However, it is known that the damping of the rubber depends on the frequency and temperature. This may explain some of the differences in the phase at low frequency. Nevertheless, this study shows that the simplified 2D axisymmetric model can calculate the magnitude and phase of the tyre mobility with reasonable accuracy.

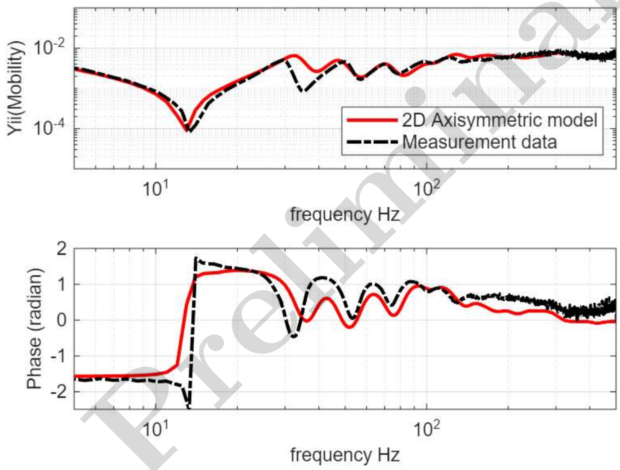

Figure 4. The mobility magnitude (top) and phase (bottom) with measurement and calculation results at the driving point.

5. Conclusion

It is demonstrated that a reduced-order axisymmetric model can overcome the limitations of conventional approaches for modelling tyre vibration in the high-frequency range without requiring excessive computational cost. Because the tyre has a multi-component structure with different principal angles, a 3D calculation model has a high computational cost. The model presented here combines certain carcass components into an equivalent orthotropic material to simplify the structure. A sensitivity analysis is used to determine appropriate material properties for these equivalent orthotropic materials by tuning the natural frequencies to measured values. The model provides a practical balance between computational efficiency and physical accuracy, making it suitable for tyre noise prediction applications.

6. Acknowledgements

The authors are grateful to Bridgestone Corporation for providing the tyre samples for use in the measurements in this study.

References

[1] S.C. Davis, R.G. Boundy: *Transportation Energy Data Book: Edition 40*. Oak Ridge: Oak Ridge National Laboratory, 2022.

[2] W. Babisch, “Road traffic noise and cardiovascular risk”, Noise & Health, Vol. 10, no. 38, pp. 27–33, 2008.

[3] B. Oftedal, N.H. Krog, A. Pyko, C. Eriksson, S. Graff-Iversen, M. Haugen, P. Schwarze, G. Pershagen, G. M. Aasvang, “Environmental Research Road traffic noise and markers of obesity – A population-based study”, Environmental Research, 138, pp. 144-153, 2015

[4] N. Mucci, V. Traversini, C. Lorini, S. D. Sio, R. P. Galea, G. Bonaccorsi, G. Arcangeli, “Urban Noise and Psychological Distress: A Systematic Review”, Int. J. Environ. Res. Public Health, 17, article 6621, 2020

[5] U. Sandberg, J.A. Ejsmont, “TYRE/ROAD NOISE REFERENCE BOOK”, INFOMEX, Harg, SE-59040 Kisa, Sweden, 2002

[6] R.J. Pinnington, “A wave model of a circular tyre. Part 1: belt modelling”, Journal of Sound and Vibration, Vol. 290, no. 1-2, pp. 101-132, 2006

[7] R.J. Pinnington, "A wave model of a circular tyre. Part 2: side-wall and force transmission modelling", Journal of Sound and Vibration, Vol. 290, no. 1-2, pp. 133-168, 2006

[8] Y. Waki, B.R. Mace, M.J. Brennan, "Free and forced vibrations of a tyre using a wave/finite element approach", Journal of Sound and Vibration, Vol. 323, no. 3-5, pp. 737-756, 2009

[9] W. Kropp, P. Sabiniarz, H. Brick, T. Beckenbauer, "On the sound radiation of a rolling tyre", Journal of Sound and Vibration, Vol. 331, no. 8, pp. 1789-1805, 2012

[10] D.J. O'Boy, A.P. Dowling, "Tyre/road interaction noise—A 3D viscoelastic multilayer model of a tyre belt", Journal of Sound and Vibration, Vol. 323, no. 4-5, pp. 270-291, 2009